3D-Modeling and Analysis of Miniature Stator Design for Electrical Machines

Aravindakshan TA[1], Philippe J. Masson[2]
1. Florida Institute of Technology, Melbourne, FL, USA
2. AML Superconductivity and Magnetics, Melbourne, FL, USA

Abstract

With the evolving trend of electrification in transportation, electric machines with higher power density and higher efficiency are demanded which results in the thermal limit of the stator winding becoming more of a key constraint. The achievable current density in stator windings is limited by ohmic and eddy current losses in the conductor. Excessive conductor heating not only limits the allowed current density, but also strains the electrical insulation needed in coils, and adversely affects the reliability and meantime-between-failure. In fact, insulation breakdown of stator windings constitutes a major failure mode of electrical machines. Since the electrical resistance of copper increases rather rapidly with temperature, effective cooling is mandatory to enable high power density and high reliability. For this study, a dual rotor permanent magnet motor is considered, allowing for the implementation of an ironless stator winding with direct cooling. Direct contact between the coolant and the conductor leads to improved cooling efficiency and current density, and enables significant overload capacity of the stator windings, facilitating, for example, the hovering phase in eVTOL aircraft applications. For many applications this should also eliminate the need for redundant phase windings thereby further increasing possible power density of the machine. A COMSOL® model was developed to simulate a sub-scale thermal mock-up of a stator design (1 pole and 1 phase) to find the peak temperature of the stator after reaching steady state and correlate it to the pressure loss across the stator. The model uses Computational fluid dynamics (CFD) and Heat transfer studies and the k-e formulation was used for solving the turbulent flow model. As part of the modelling, a parametric analysis was performed to study the effects of the peak temperature of the stator for different mass flow velocities of air and current densities. Air is used as the working fluid and PEEK and Alumina are used as stator possible support material. A Litz wire with a filling factor of 0.7 is used as the conductor to minimize the eddy currents in the stator due to high frequency magnetic field. COMSOL Multiphysics® was used in this study because of its ability to perform multiphysics simulations, handle highly non-linear problems and its parametric analysis capabilities. As a follow up study, the simulation results will be compared to measurements performed on a sub-scale mock-up stator winding.

Introduction

Electrical machine design is constrained by three main factors, namely the electromagnetic, the mechanical and the thermal limits. The demand for higher power and torque densities, enabled by advances in materials and design tools, is resulting in the thermal limit nowadays becoming more and more the dominant constraint. For this reason, appropriate thermal management is required for avoiding over-temperatures. An advantage resulting from lowering the winding temperature is represented by the reduction of the winding's electrical resistance, which leads to lower copper losses for a given current density [1]. A proper thermal management allows higher current densities for a given winding temperature limit (which depends on the insulation thermal class), which can result in higher torque for the same machine's size. As a rule of thumb, a 10°C increase in temperature halves the insulation system lifetime [2,3].

Conventional air-cooling systems, such as shaft-mounted fans, housing fins or external fans, are very effective. However, for high power density machines, with elevated current densities, they may not be enough to guarantee adequate cooling, especially in the center of the stator slots or coils. The difficulty with conventional shaft-mounted fans is that as the machines are loaded and the as the RPM decreases, i.e. the losses increase while at the same time the fan performance decreases and thus the mass flow rate goes down as well. Consequently, advanced cooling methods, employing either high thermal conductivity fluids or high thermal conductivity insulation materials, have recently also become popular.[4]

A common technique for cooling improvements is using forced liquid cooling methods involving channels, ducts or water jackets. Such methods provide excellent cooling within the active region of windings [5]. However, very often they do not have the same effect towards the end-windings, resulting in the hot spot being localized in this area of the machine.

In this paper a direct cooling method is used, and air is in direct contact with the stator winding by flowing over the conductor. The stator design is for a dual rotor motor and figure1 shows an example of one. For the analysis, 1 pole and 1 phase of the stator is modelled and this study; this is the first step in validating the thermal design experimentally. This paper also compares the performance of two-stator materials PEEK and Alumina and by looking at the stator peak temperature for the same flow conditions. Then a parametric analysis is performed looking at peak temperature and pressure drop for different velocities and current density combinations.

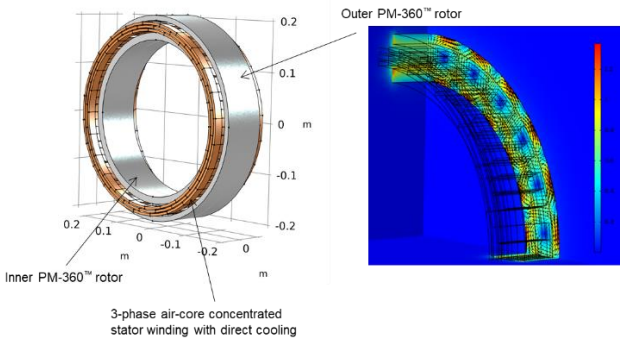

Figure 1. Example geometry for a dual rotor motor based on AML's PM-360 magnets (left) and magnetic flux distribution (right)

Numerical Model

The geometry is a miniature stator design (1 pole and 1 phase) and is composed of two layers of copper (conductor) sitting on a support structure separated by an air gap. Both PEEK and Alumina are simulated as the support structure materials and their impact on peak temperatures is compared and analyzed. The geometry of the miniature stator design is shown below in figure 2 and the air domain is shown in figure 3.

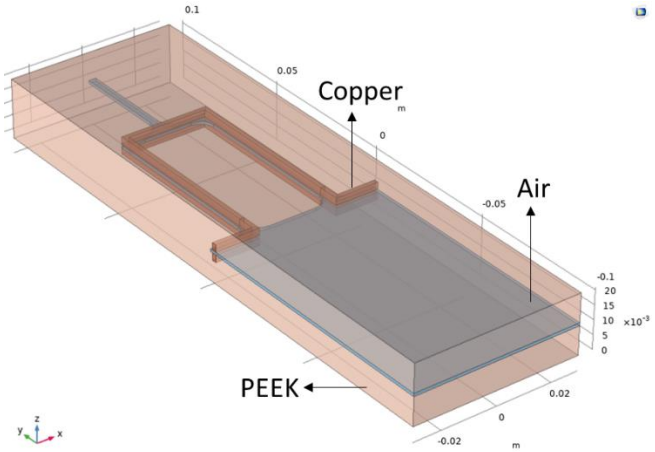

Figure 2. Geometry of miniature stator with 1 pole and 1 phase

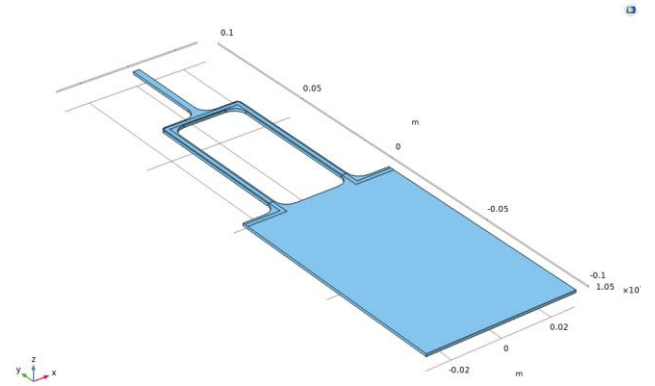

Figure 3. Air Domain

The PEEK support substrate is 60 mm X 200 mm X 21 mm and the air gap is 1 mm. The copper is 388 mm long and the cross-section of the copper is 1.6 mm X 2.5 mm. The inlet air flow cross-section is 60 mm X 1 mm and the outlet cross-section is 2.6 mm X 1 mm.

The properties for air, copper, PEEK and Alumina were imported from the COMSOL materials library. The thermal conductivity and heat capacity at constant pressure for PEEK are 0.25 W/m.K and 320 J/Kg.K respectively and were added to the properties list. Alumina has a thermal conductivity of 25 W/m.K and the specific heat is 880 J/Kg.K.

The simulation requires coupling of the k-e turbulent flow and the heat transfer in solids and fluids multiphysics. The governing equations for these models are the Navier-Stokes and the k-e equations and are solved to obtain the components of the fluid velocity. The continuity and momentum equations for an incompressible flow is given by equation 1 and 2 respectively.

$$\nabla.(\rho u) = 0 \tag{1}$$

$$\rho(u.\nabla)u = \left[-pI + (\mu + \mu_T)(\nabla u + (\nabla u)^T) - \frac{2}{3}\mu(\nabla.u)I\right] + F \tag{2}$$

In the above equations u is the fluid velocity vector, ρ is the fluid density, μ is the fluid viscosity and μ_T is the turbulent viscosity and F is the body forces present. Turbulent viscosities are the effects of the small-scale time-dependent velocity fluctuations.

In all numerical analysis, the accuracy of the results is dependent on the turbulent models used, near-wall treatments applied, discretization schemes employed, convergence criteria set and other solver settings. In this study the standard k-ε turbulence model is used and is often used in industrial applications because it is both robust and computationally inexpensive. It consists of solving two additional equations for the transport of turbulent kinetic energy k and turbulent dissipation ε and is shown in equation (3) and (4).

$$\rho(u.\nabla)k = \nabla.\left[\left(\mu + \frac{\mu_T}{\sigma_k}\right)\nabla k\right] + P_k - \rho\varepsilon \tag{3}$$

$$\rho(u.\nabla)\varepsilon = \nabla.\left[\left(\mu + \frac{\mu_T}{\sigma_\varepsilon}\right)\nabla\varepsilon\right] + C_{\varepsilon 1}\frac{\varepsilon}{k}P_k - C_{\varepsilon 2}\rho\frac{\varepsilon^2}{k} \tag{4}$$

$$\mu_T = \rho C_\mu \frac{k^2}{\varepsilon} \tag{5}$$

In the above equations $\sigma_\varepsilon, \sigma_k, C_{\varepsilon 1}$ and $C_{\varepsilon 2}$ are adjustable constants and the values of these are obtained from numerous iterations of data fitting for wide range of turbulent flows and are available in literature. The k- ε formulation is usually useful for free-shear layer flows with relatively small pressure gradients as well as in confined flows where the Reynolds shear stresses are most important

The Navier stokes energy equation is used to solve for the temperature of the fluid and is given by equation 6.

$$\rho C_p u.\nabla T = Q + \nabla(k\nabla T) \tag{6}$$

C_p is the specific heat at constant pressure of the fluid, Q is the external heat source, k is the thermal conductivity of the fluid and T is the temperature of the fluid.

Boundary Conditions (BCs) have a key role in solving the Partial Differential Equations (PDEs). For this model, the BCs are velocity inlet (Equation 7) and a pressure outlet (Equation 8) with the air flow in the positive y direction.

$$u = -u_0 n \tag{7}$$

$$[-pI + K]n = -\hat{p}_0 n \tag{8}$$

The rest of the surfaces in the fluid domains are walls and are assigned the no slip boundary condition.

The no slip condition equation is given by equation (9).

$$u = 0 \tag{9}$$

There is thermal insulation on the top, bottom, left, right, inlet and outlet sides of the channel and thermal insulation equation is given by equation (10).

$$-n.(k\nabla T) = 0 \tag{10}$$

The temperature gradient across the boundary must be zero and thus the temperature on either side of the surface must be equal and thus no heat is transferred.

The copper litz wire is the heat source for the stator. So, for a given current density of the stator wire the power density is calculated as shown in equation (11).

$$Q_0 = f.\rho_r J^2 * volume \tag{11}$$

In the above equation *f* is the filling factor of the litz wire which is equal to 0.7 for the analysis, according to the manufacturer specifications. ρ_r is the resistivity of the wire material and *J* is the current density and Q_0 is the power density in W/m^3. The initial values for the velocity and temperature are (u,v,w) = (0,1.5,0) and T_0 = 298 K and *u*, *v*, *w* are the three components of velocity in the *x*, *y* and *z* direction respectively.

Mesh

Mesh generation is one of the most important steps of the any numerical analysis. After geometry definition, it is necessary to subdivide fluid domain into several smaller, non-overlapping sub-domains and this results in a mesh of cells. The equations that describe flow properties are numerically solved in each of the defined mesh cells. A larger number of cells generally leads to a more accurate solution, but it can be more restrictive to model larger systems, since it needs more computation resources that are not always available. Thus, a mesh independence study has been performed and the volume average temperature of the stator is evaluated for increasing number of elements. Figure 5 shows that the curve starts flattening out around 1.2 million elements. This means that

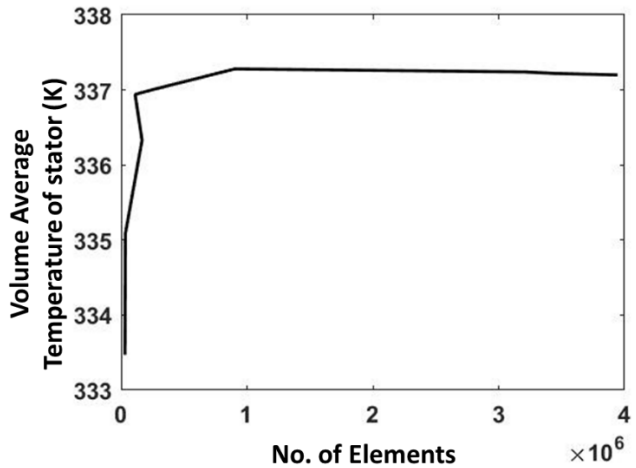

Figure 4. Mesh Independence Study

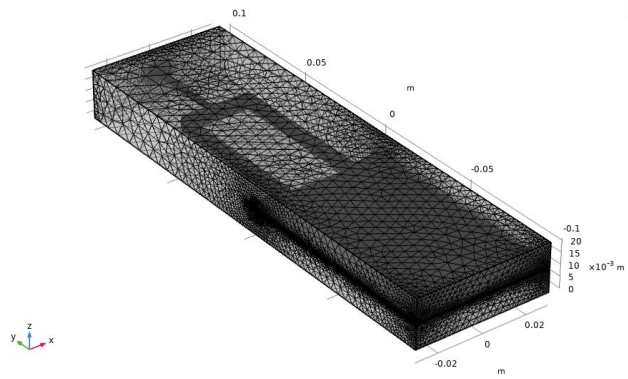

Figure 5. Sample Mesh

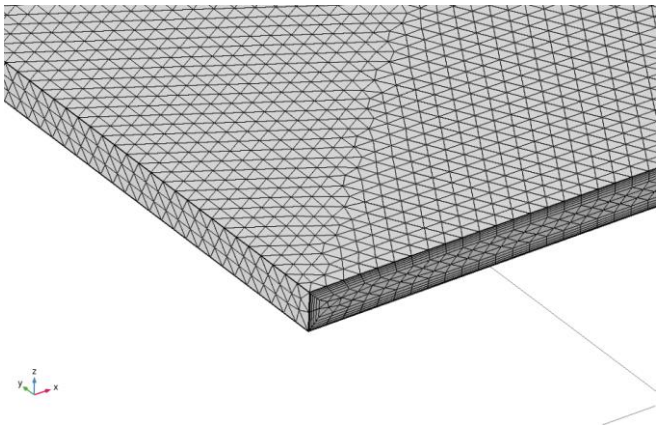

Figure 6. Fluid Domain Mesh

increasing the number of elements further will not improve the solution accuracy and thus 1.2 million elements is the target when meshing the models. The mesh used for the simulations is shown in figure 5 and has 1209210 elements. The fluid domain is shown in figure 6, with the domain having 506675 elements and the number of boundary layers is 6 with boundary layer stretching factor of 1.2.

Results

Using the turbulent flow with k-ε formulation and heat transfer in solids and fluids, the stationary study is simulated in COMSOL. For the initial analysis, a velocity inlet of 1.5 m/s and a litz wire current density of 20 A/mm^2 is used with PEEK used as the support material. Figure 7,8 and 9 shows the velocity, pressure, and temperature profiles for the stator design. Figure 6 shows the velocity increasing to 23 m/s when the channel narrows down near the copper wire. With an increase in velocity the Reynolds number increases and thus there is more turbulence which ultimately increases the heat transfer coefficient and helps with better heat transfer. The peak temperature of the stator is 422 K and the pressure drop across the stator is 1935 Pa. For the next analysis, the same velocity inlet and current density boundary conditions are used, but the only difference is the support material is alumina instead of PEEK. Since the flow boundary conditions are the same, the velocity and the pressure drop profile are the same to that of the PEEK.

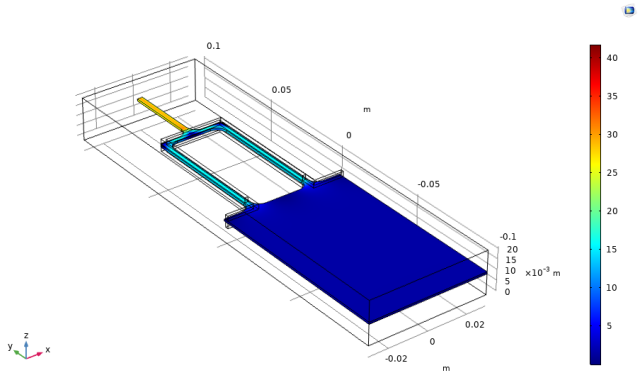

Figure 7. Velocity Profile

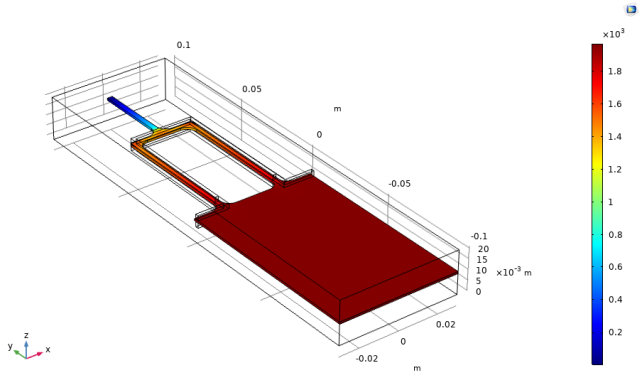

Figure 8. Pressure Profile

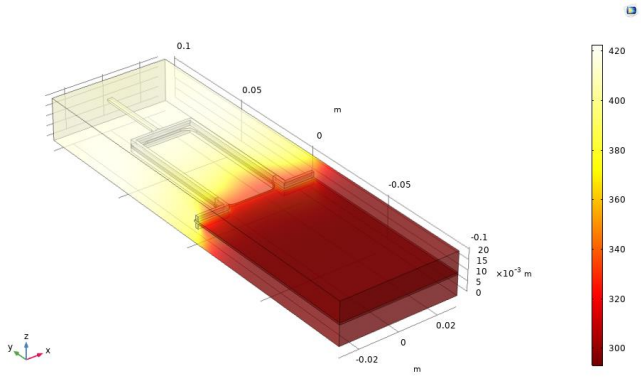

Figure9. Stator Temperature Profile (PEEK)

However, there is a difference in the peak temperature and is 404 K when Alumina is the substrate. Alumina has a thermal conductivity 100 times greater than PEEK and this leads to better heat transfer in the case of Alumina and thus the peak temperature is lower. Figure 10 shows the temperature profile for Alumina and it can be seen the gradient is uniform after reaching steady state when compared to that of PEEK. In terms of material for the stator support structure and looking at the performance thermally, Alumina is better than PEEK due to the fact the peak temperature is lower for Alumina and there are no hotspots in the stator.

Following the analysis on two different stator material a parametric analysis was set up to study the effects of velocity and current density on peak temperature and pressure drop across the stator. The inlet velocity is varied from 1.5 m/s to 5m/s with a step size of 0.5 m/s and the current density has been varied from 20 A/mm^2 to 30 A/mm^2 with a step size of 2 A/mm^2.

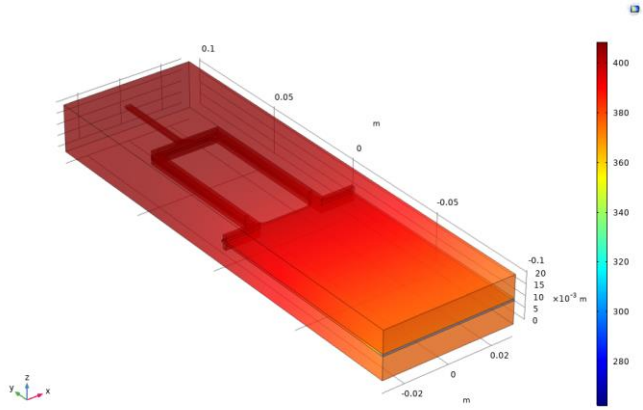

Figure 10. Stator Temperature Profile (Alumina)

All the different 48 combinations were simulated, and the results are summarized in figures 11,12,13 and 14. Figure 11 shows the variation of Max Stator temperature for increasing inlet velocities when the current density is 20 A/mm^2. As velocity increases the Reynolds number increases as well and is shown in equation (12)

$$Re_D = \frac{\rho . V . D_h}{\mu} \qquad (12)$$

In equation 12, Re_D is the Reynolds number, V is the flow velocity, D_h is the hydraulic diameter and μ is the dynamic viscosity. The convective heat transfer coefficient is the parameter which determines the quality of heat transfer. Higher the heat transfer coefficient better the heat transfer. The convective heat transfer coefficient is found using equation (13):

$$h = Nu \frac{k}{D_h} \qquad (13)$$

In equation (13), Nu is the Nusselt number and k is the thermal conductivity of the fluid. Nusselt number is function of Reynolds number and Prandtl number and there are many correlations for Nusselt number for the turbulent flow regime and the appropriate correlation is picked based on the geometry and Prandtl number range. Generally, the Nusselt number increases with increase in Reynolds number and that leads to a higher heat transfer coefficient which means better heat exchange and thus lower peak temperature.

As the inlet velocity increase from 1.5 to 5 m/s the peak temperature decreases by 16%. Figure 12 shows a surface plot explaining the effects of peak temperature when both the inlet velocity and the current density is varied. When current density increases the heat generated also increases as shown in equation 11. Thus, for the same velocity with increase in current density the peak temperature of the stator increases as well. When the stator current density increases by 50 % the peak temperature increases by 41%. Pressure drop is an important performance parameter for the stator and a high-pressure loss adds to the pumping costs. Figure 13 shows the variation in pressure drop across the stator for increasing inlet velocities. The pressure drop is directly proportional to the frictional factor and the velocity.

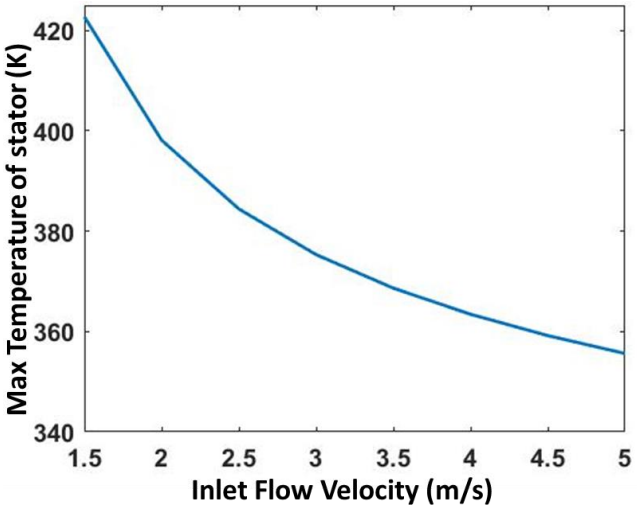

Figure 11. Inlet velocity vs Max Stator Temperature

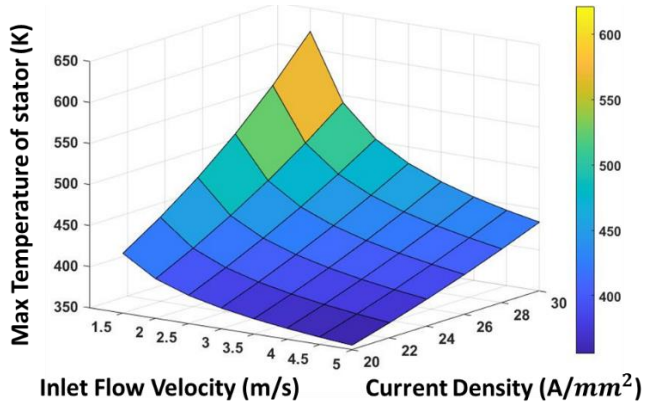

Figure 12. Surface Plot showing the Variation in Max Stator Temperature with Velocity and Current Density

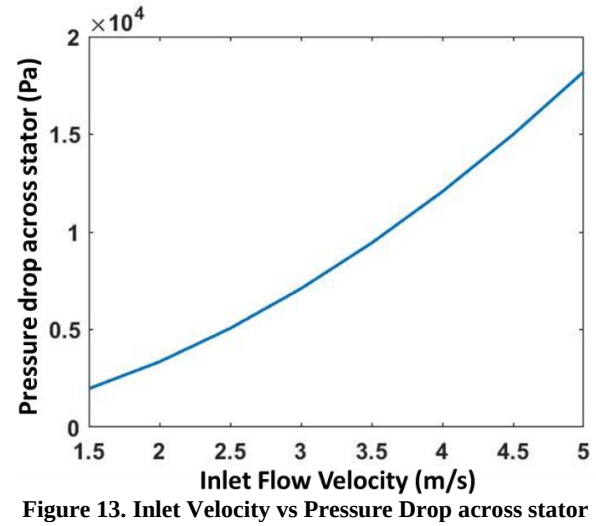

Figure 13. Inlet Velocity vs Pressure Drop across stator

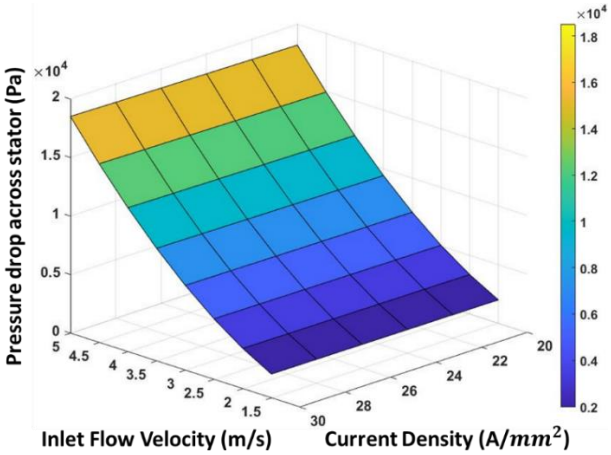

Figure 14. Surface Plot showing the Variation in Pressure Drop across the Stator with Velocity and Current Density

As velocity increases the Reynolds number and frictional factor increases as well. As the inlet velocity increase from 1.5 to 5 m/s the pressure drop increases by 810%. Figure 14 shows a surface plot representing the changes in pressure drop across the stator when both the inlet velocity and the current density of the wire is varied. Thus, for the same velocity with increase in current density the pressure drop across the stator increases marginally. When the stator current density increases by 50 % the pressure drop across the stator increases by 3%. This small change is due to the density and dynamic viscosity changing with temperature which in turn affects the pressure drop. There is a tradeoff between the pressure drop and the peak temperature of the stator. Thus, both temperature and pressure drop are critical performance parameters when designing stators for different applications.

Conclusions

The simulation results demonstrate that when using Alumina as the stator support material the peak temperature was 5% lower when compared to PEEK as support material for the stator. The reason being the thermal conductivity of Alumina is 10 times higher than that of PEEK and thus heat transfer is better. A parametric analysis was performed showing higher the velocity leads to a decrease in peak temperature. It was shown that as the inlet velocity increase from 1.5 to 5 m/s the peak temperature decreases by 16%, but the tradeoff is pressure loss which increases by 810%. The effects of current density were also analyzed and for a 50% increase in current density of the conductor, the peak temperature increases by 41%. The pressure drop change is minimal as the flow conditions do not change and only the thermal properties of the material changes due to the increase in temperature leading to 3% increase in pressure drop. This steady state thermal analysis provides valuable guidance for designing such stator configuration and acts as a good base for future experimental tests and validations. The miniature stator will be fabricated and tested to validate the design experimentally.

References

1. Y. Yang, B. Bilgin, M. Kasprzak, S. Nalakath, H. Sadek, M. Preindl, et al., "Thermal management of electric machines," IET Electrical Systems in Transportation, vol. 7, pp. 104-116, 2017.

2. S. Grubic, J. M. Aller, B. Lu, and T. G. Habetler, "A Survey on Testing and Monitoring Methods for Stator Insulation Systems of Low-Voltage Induction Machines Focusing on Turn Insulation Problems," IEEE Trans. on Ind. Electron., vol. 55, pp. 4127-4136, 2008.

3. C. Sciascera, M. Galea, P. Giangrande, and C. Gerada, "Lifetime consumption and degradation analysis of the winding insulation of electrical machines," in 8th IET International

Conference on Power Electronics, Machines and Drives (PEMD 2016), 2016, pp. 1-5.
4. M. Popescu, D. A. Staton, A. Boglietti, A. Cavagnino, D. Hawkins, and J. Goss, "Modern Heat Extraction Systems for Power Traction Machines - A Review," IEEE Transactions on Industry Applications, vol. 52, pp. 2167-2175, 2016.
5. M. Galea, C. Gerada, T. Raminosoa, P. Wheeler, , "Design of a high force density tubular permanent magnet motor," in The XIX Int. Conf. Elec. Mach.(ICEM'2010), Rome, Italy, 2010, pp. 1-6.